HHS Public Access

Author manuscript

Gene Ther. Author manuscript; available in PMC 2016 March 01.

Published in final edited form as:

Gene Ther. 2015 September ; 22(9): 739–749. doi:10.1038/gt.2015.36.

Ultrasound-assisted non-viral gene transfer of AQP1 to the irradiated minipig parotid gland restores fluid secretion

Z Wang[1], **L Zourelias**[1], **C Wu**[1], **PC Edwards**[2], **M Trombetta**[3], and **MJ Passineau**[1]

[1]Gene Therapy Program, Department of Medicine, Division of Cardiovascular Medicine, Allegheny Health Network, Pittsburgh, PA, USA

[2]Department of Oral Pathology, Medicine and Radiology, University of Indiana School of Dentistry, Indianapolis, IN, USA

[3]Department of Oncology, Allegheny Health Network, Division of Radiation Oncology, Allegheny General Hospital, Pittsburgh, Pa, USA

Abstract

Rationale—Xerostomia is a common side effect of ionizing radiation used to treat head and neck cancer. A groundbreaking Phase I human clinical trial utilizing Adenoviral gene transfer of Aquaporin-1 (AQP1) to a single salivary gland of individuals suffering from radiation-induced xerostomia has recently been reported. Unfortunately, the limitations of the Adenoviral vector system utilized in this pioneering trial preclude its advancement to a Phase II trial and we have thus undertaken to evaluate the therapeutic potential of ultrasound-assisted non-viral gene transfer (UAGT) as an alternative means of delivering AQP1 gene therapy to the salivary gland by comparing head-to-head with the canonical Adenoviral vector in a swine model.

Findings—Swine irradiated unilaterally with a 10Gy electron beam targeted at the parotid gland suffered from significant, sustained hyposalivation that was bilateral, despite irradiation being confined to the targeted gland. Unilateral AQP1 gene therapy with UAGT resulted in bilateral restoration of stimulated salivary flow at 48 hours and one week post-treatment (1.62+/−0.48ml, 1.87+/−0.45ml) to pre-injury levels (1.34+/−0.14ml) in a manner comparable to Adenoviral delivery (2.32+/−0.6ml, 1.33+/−0.97ml).

Conclusions—UAGT can replace the Adenoviral vector as a means of delivering AQP1 gene therapy in the irradiated swine model and is a candidate for advancement to a Phase I human clinical trial.

Address for correspondence: Michael J Passineau, PhD, Director, Gene Therapy Program, Allegheny Health Network, Room 841, South Tower, 320 East North Avenue, Pittsburgh, PA 15212-4772, 412-359-6557 (voice), 412-359-4698 (fax), mpassine@wpahs.org.

Conflict of Interest

The authors declare no conflict of interest.

Introduction

Cancers of the head and neck (HNC) comprise roughly 3% of all cancer cases in the United States (1), with an incidence estimated at 52,000 cases in the United States in 2013(2). Incidence of these cancers varies globally, according to the prevalence of risk factors in various populations. Throughout the developed world, external beam radiation remains a mainstay of therapy for most types and stages of HNC, either alone or in combination with surgery and/or chemotherapy. Coirradiation of the salivary glands during radiotherapy is common and results in severe and irreversible hyposalivation, which in turn leads to a constellation of oral morbidities including xerostomia and dental disease (3).

Treatment options for radiation-induced xerostomia are extremely limited and consist of exogenous rehydration and management of progressive damage to the oral mucosa and dentition. In light of these limited treatment options and the chronic and debilitating nature of this condition, gene therapy for radiation-induced xerostomia has been developed and successfully demonstrated in a Phase I clinical trial (4, 5). This gene therapy strategy is targeted to the ductal cells of the salivary gland which, in contrast to the saliva-producing acinar cells, are resistant to ionizing radiation and survive radiotherapy largely intact. Using an Adenoviral vector to express Aquaporin 1 (AdAQP1) in parotid gland ductal cells, Baum and coworkers developed a treatment paradigm (5) that results in the transcellular flux of interstitial fluid across the ductal cell layer and into the intraductal labyrinth of the salivary gland, where the fluid can be expelled to produce palliative oral wetness.

This AdAQP1 clinical trial has successfully established the safety of AQP1 gene therapy, as well as demonstrating objective improvements in parotid salivary flow rates and subjective improvement in xerostomia in patients receiving the treatment in a dose-dependent manner. Despite this remarkable success, a Phase II trial of AdAQP1 is not planned, as the therapeutic effect is transient and this vector is not suitable for the readministration required to treat this chronic condition. Adenovirus elicits strong host immune response in humans, and this response is thought to be progressive with repeated exposure (6, 7). In the aggregate, successful application of AQP1 gene therapy in radiation-induced xerostomia is dependent upon the clinical implementation of a gene therapy technique that evades host immune response and allows for periodic readministration throughout the lifetime of the individual.

Our efforts toward this goal have focused on ultrasound-assisted gene transfer (UAGT) to the salivary gland, which combines the use of a non-viral DNA vector and lipid/perflutren microbubbles with a low frequency acoustic field to create a “sonoporation” effect, allowing gene transfer to the cells of the salivary gland without the introduction of viral antigens. This method has been shown to successfully express transgenes within the salivary gland of rodents (8, 9), and has advantages over conventional viral vectors. Most notably, this method utilizes three safe and clinical-grade components: 1) clinical ultrasound, 2) perflutren lipid microbubbles which have been approved for intravascular administration to humans (10), and 3) plasmid DNA vectors. While intracellular host immune response can still occur with non-viral DNA vectors (9), extracellular host response, either humoral or

cell-mediated, is thought to be minimized in the absence of viral antigens, provided that the transgene itself is native to the host.

This report describes our efforts to develop and characterize a swine model of radiation-induced xerostomia, to effect UAGT to the parotid gland of swine subjects, and ultimately to compare the therapeutic efficacy and duration of AQP1 gene therapy in the swine using UAGT and Adenoviral gene transfer head-to-head. As the swine is the penultimate preclinical model of radiation-induced xerostomia, our efforts were designed to mimic those of the AdAQP1 preclinical development effort (11), and to potentially provide a rationale for the translation of UAGT/AQP1 to a Phase I clinical trial in patients suffering from radiation-induced xerostomia. If successful, these efforts could provide an alternative to viral-based gene therapy, and, by obviating host immune response, establish a gene therapy protocol that could be periodically re-administered throughout the lifetime of the patient.

Results

Figure 1 illustrates, in graphical and table format, the experimental groups utilized in this study and the treatments, sample collections, and experimental endpoint of each group.

A single 10Gy dose of radiation delivered by an electron beam to the right parotid gland results in significant, sustained, and bilateral hyposalivation in the miniature swine

The digitally reconstructed radiograph (DRR) image used to treatment plan the electron beam for all study subjects is shown in Figure 2A. In order to confirm that the control gland received no radiation, we placed thermo-luminescent detectors on the skin overlying the right (treated) and left (control) parotid gland during the application of the electron beam. Figure 2B shows that the control gland received no detectable radiation.

A baseline stimulated, isolated parotid saliva collection was performed on all animals (n=16), bilaterally and immediately prior to irradiation (approximately 10 weeks of age) and at 4, 6, 8, 10, and 12 weeks post-irradiation. Saliva volume was determined by weight, assuming a specific gravity of 1.0. Figure 2C shows stimulated parotid saliva volumes for the irradiated (right) and control (left) sides. Notably, despite the demonstrated lack of radiation damage to the control gland, saliva output of the control side began to decline from baseline by Week 8, decreasing further at Week 10 and Week 12. Our conservative statistical strategy did not find significant differences between Baseline and Control to support the visually obvious trend, but suggested Control and Irradiated were changing over time at similar rates. These finding suggest a functional coupling of the right and left parotid glands, which we suspect has a neurological basis.

Ultrasound-assisted gene transfer of met-Luc to the irradiated salivary gland produces bioluminescent saliva but no increase in stimulated saliva volume

Our group has previously reported ultrasound-assisted gene transfer via “sonoporation” in the mouse salivary gland (8), but to our knowledge, the application of this technology to the salivary gland of the swine has never been reported. Demonstrating this phenomenon in the pig proved challenging since the size of the animal precludes the use of the conventional IVIS imaging technique we had previously relied upon. We therefore turned to the secreted

Metridia longa luciferase (MetLuc) reporter gene (12), reasoning that if we were successful in accomplishing expression of this reporter gene in the pig's salivary gland, we should be able to detect luminescence in the saliva secreted from a salivary gland thus treated. Figure 3A shows the results of a MetLuc assay performed on stimulated saliva collected from the Irradiated/MetLuc-treated (right) side 48 hours after UAGT, compared with the control (left) side. These results demonstrate, for the first time, ultrasound-assisted non-viral gene transfer to the salivary gland of adult swine and also illustrate the precise isolation of saliva collected from individual parotid glands, with no detectable mixing of samples from the treated (right) and control (left) glands.

This experiment served a second purpose; that of a negative control for ultrasound-assisted AQP1 gene therapy, described below. Pigs receiving MetLuc via UAGT underwent exactly the same manipulation as animals receiving either Adenoviral or ultrasound-assisted AQP1 gene therapy as described below. Stimulated saliva volumes collected immediately prior to, and 48 hours after, UAGT with MetLuc (Figure 3B), demonstrate that there is no effect of the UAGT methodology *per se*, on stimulated parotid saliva volume.

Xerostomia in our swine model is reversed by the clinically validated Adenovirus expressing human AQP1 (hAQP1)

The intent of this study was to measure AQP1 gene therapy delivered by UAGT against the clinical standard, AQP1 delivered by Adenovirus. Human AQP1, delivered by a viral vector, has previously been utilized as a gene therapy for xerostomia in the rat (13), the swine (14), and ultimately humans (4). Thus, we first sought to demonstrate that our swine model of radiation-induced xerostomia responds to Adenoviral gene therapy in a manner consistent with what was previously reported in the canonical study by Shan *et al* (14). We obtained a non-clinical grade prep of the AdhAQP1 virus from the NIH team (a kind gift of Dr. Changyu Zheng, NIDCR) to ensure that we were utilizing the same vector that has shown therapeutic efficacy in the human clinical trial.

Consistent with earlier preclinical work utilizing AdhAQP1 in the swine model our animals received 1×10^{10} viral particles (vp) of the vector to the irradiated gland, 12 weeks following irradiation (n=4). AdhAQP1 reverses hyposalivation in our swine model (Figure 4) in a manner similar to that reported by Shan *et al*. Further, gene therapy delivered to the irradiated gland was observed to substantially enhance stimulated fluid secretion from the contralateral gland, lending additional support for functional coupling between the left and right parotid glands. The extinction of the therapeutic effect within two weeks is consistent with the known gene expression dynamics of the Adenoviral vector in mammals.

Porcine AQP1(pAQP1) expressed in MDCK cells results in transcellular water permeability

The above experiment demonstrates that our swine model responds to AdhAQP1 gene therapy in a manner similar to the earlier swine model that utilized unilateral irradiation with photons. However, since our UAGT or "sonoporation" gene transfer technology obviates the need for a viral vector, and thus avoids the introduction of foreign antigens into the damaged salivary gland, we decided to carry our experiments forward with porcine AQP1 (pAQP1). Our clinical translational goal is to use UAGT to express hAQP1 in human salivary glands,

and thus modeling that goal using pAQP1 in pigs seems a sound way of determining the duration of therapeutic effect following UAGT, absent concerns of host response against a foreign transgene (i.e. hAQP1), which could of themselves limit the duration of therapeutic effect.

pAQP1 was cloned as described in Material and Methods and expressed by plasmid transfection into MDCK canine kidney epithelial cells plated as a monolayer in transwell chambers (Figure 5A). Compared to GFP-transfected cells, cells transfected with pAQP1 showed enhanced water flux across the monolayer (Figure 5B). These experiments demonstrate the physiological functionality of our pAQP1 transgene product.

Porcine AQP1 gene therapy delivered to the irradiated salivary gland with UAGT increases stimulated salivary flow to levels comparable with Adenoviral gene therapy

With this preparatory work completed, we next undertook to test our main hypothesis that UAGT of pAQP1 to the irradiated gland can increase stimulated parotid saliva volume in a fashion similar to that previously demonstrated with hAQP1 delivered by an Adenovirus. Increases in stimulated parotid saliva volume were observed in both treated and control sides in UAGT/pAQP1 treated-animals (n=4, Figure 6), with the magnitude of the increase being roughly comparable to that seen with the AdhAQP1 virus in this model. A similar bilateral effect was also observed, despite the fact that gene therapy was delivered only to the irradiated side. The increases in saliva volume declined substantially by 2 weeks post-treatment, showing a trend toward persistent therapeutic effect on the control side but no longer statically different from pre-treatment levels. Notably, function improved markedly in the control gland despite the fact that gene therapy was only delivered to the irradiated gland.

UAGT does not promote the local inflammation observed with Adenoviral gene transfer to the salivary gland

The major factor limiting the clinical utility of Adenoviral gene therapy in chronic conditions like xerostomia is the vector's robust immunogenicity; a phenomenon that has previously been described histologically in the salivary gland (15–17), even with UV-inactivated Adenoviral particles, suggesting it is mediated entirely by the viral capsid (18). Further, systemic inflammation resulting from Adenoviral gene transfer to the salivary gland, as indicated by chronic inflammatory focal lesions and induction of anti-Adenoviral antibodies have also been reported (18, 19). As our UAGT technique accomplishes gene therapy that is comparable to Adenovirus-mediated gene transfer, but obviates the introduction of viral antigens into the subject's body, we hypothesized that UAGT would also minimize local and systemic inflammatory response.

In order to test this hypothesis, we constructed an Adenoviral vector expressing the pAQP1 cDNA described above. We treated a group of swine (n=4, Group 4), irradiated on the right side as described above, with this AdpAQP1 and sacrificed this group 1 week after gene transfer. The UAGT/MetLuc negative control animals (n=4, Group 3), described previously, were sacrificed 1 week after gene transfer and served as the UAGT control. In all experiments, the unirradiated (left) parotid gland was left untouched and served as an

internal control for each animal. The design of this experiment was such that we could determine the effects of Adenoviral gene delivery relative UAGT upon the histology of the parotid gland.

Slides were reviewed by an oral pathologist (PCE) blinded as to experimental design and animal identities. Results of this experiment are summarized in Table 1 and representative sections are shown in Figure 7. Relative to control glands, two primary histological findings were noted. First, mild acinar cell pleomorphism and changes in zymogen granules were observed in all irradiated glands (Figure 7 panels 7B, 7D, 7F, 7H). The second finding was interstitial and periductal inflammation, which was restricted to glands treated with the Adenoviral vector (Figure 7 panels 7F, 7H). Importantly, UAGT had no detectable effect upon the structure or morphology of the salivary gland, reinforcing the safety of this technique relative to the canonical Adenoviral vector.

Saliva produced by the damaged parotid gland after gene therapy shows a profile very similar to normal saliva, but with the loss of select proteins of putative acinar origin

Aquaporin-1 gene therapy as a treatment for radiation-induced xerostomia is predicated upon the simple mechanism of transcellular movement of fluid via AQP1 across surviving ductal cells. This is not fundamentally different from normal physiological salivation, which utilizes primarily Aquaporin-5 to drive transcellular fluid movement across acinar cells (20). In both instances, the source of the bulk of this fluid is ultimately the interstitium, which in turn is mainly dependent upon the serum for its protein composition (21). Accordingly, we explored to what degree the proteome of “saliva” produced as a result of our gene therapy would differ from natural saliva.

To investigate this issue, we performed proteomic profiling using difference gel electrophoresis (DiGE) on matched samples of saliva obtained 48 hours after gene therapy from the right (irradiated, treated) and left (control, untreated) parotid glands within the same animal relative to baseline saliva collected and banked from the same animal prior to irradiation. In order to evaluate the quality of this saliva in the most clinically meaningful way, saliva obtained from the treated and control parotid glands were indexed to baseline saliva. Figure 8 shows composite proteomic profiles of saliva at baseline, from the control gland, and from the gene therapy-treated gland. The global similarity of Baseline and Control saliva relative to UAGT/pAQP1 saliva is visually evident (Figure 8A, 8B versus 8C).

Biological Variation Analysis (BVA) was performed using the DeCyder platform, and we found the following differences: Baseline versus Control, 152 of 2253 matched spots significantly changed ($p<0.05$), and Baseline versus Treated, 186 of 2362 matched proteins significantly changed ($p<0.05$). In order to evaluate the potential clinical significance of salivary proteins lost as a result of radiation injury to the parotid gland, we selected and extracted spots determined to be significantly altered in UAGT/pAQP1 saliva versus Baseline saliva, but not significantly altered in Control versus Baseline saliva (a manual step confirmed this as a check on the software). Of the 108 spots extracted, 71 were positively identified using mass spectrometry, and results are shown in Table 2.

Discussion

The development of salivary gland gene therapy from proof of concept in 1994(22) through to successful Phase I human clinical trial in 2013(4) is one of the finest examples of translational gene therapeutics yet reported. While xerostomia is not life threatening or life limiting, the impact of this condition on quality of life, nutrition, oral and digestive health is severe and can be devastating (23). When it is considered that patients suffering from radiation-induced xerostomia, as well as other causes of xerostomia such as Sjogren's syndrome and drug-related xerostomia, can live for decades with this condition, the development of a clinically practicable salivary gland gene therapy has the potential to mitigate the suffering of millions of people.

The present study is the first to show that UAGT can provide effective gene therapy for radiation-induced xerostomia in the penultimate preclinical model, the irradiated miniature swine. We have developed and now report a novel swine model wherein irradiation of the salivary gland is accomplished with an electron beam, obviating the possibility of radiation damage to the contralateral gland. Based upon this model, we report a novel observation that unilateral damage to one parotid gland impairs the function of the contralateral gland. This mechanism should be considered in interpreting the results of the AdhAQP1 Phase I clinical trial.

The observation that the functions of the left and right parotid glands are functionally coupled is interesting and likely of great clinical importance. Two previous studies in a similar irradiated pig model noted possible reduction in salivary flow from the uninjured gland (14, 24), but as these studies utilized photons, it was assumed that the contralateral effects were due to some spillover and/or scatter of radiation from the targeted side. In our study, that possibility has been excluded, demonstrating that the reduction in flow on the contralateral side is related in some way to damage to the targeted gland. There is evidence of a neurological interplay between different salivary glands in rats (25), albeit this is not well characterized. Interestingly, one study showed that unilateral parotid irradiation was sufficient to ameliorate sialorrhea in patients suffering from amyotrophic lateral sclerosis (26).

To our knowledge, this study is the first to demonstrate non-viral UAGT to the parotid glands of swine. Our technique delivers therapeutic benefit equivalent to the clinically-validated Adenoviral gene therapy approach, but obviates the need to expose the patient to the systemic toxicity and local inflammation associated with the Adenoviral vector. This host immune response to viral vectors has historically presented the greatest challenge to the mainstreaming of gene therapy, and in the case of gene therapy for radiation-induced xerostomia, this limitation makes Adenovirus unsuitable for advancement to a Phase II trial. Histometrics of damage to the salivary gland resulting from Adenoviral gene transfer have not been evaluated in humans, but significant morphological and functional damage to the salivary glands following Adenoviral gene transfer has been noted in animal studies (15, 16, 18) and we now report data confirming these safety considerations. Alternative strategies, such as Adeno-associated virus (AAV) delivery of AQP1 are being evaluated, but would

still necessarily involve re-exposing the patient to a viral vector every few years, risking progressive anti-vector host response (27–30).

The proteome of the fluid produced as a result of our gene therapy intervention is qualitatively very similar to natural saliva but lacks certain proteins normally supplied by the parotid acinar cells (see (31) for a global overview of this topic). The clinical significance of this observation is complex and not yet entirely clear. On the one hand, there is no doubt that the fluid produced is likely to be palliative, and can be expected to relieve subjective xerostomia in patients, as it is reported to have done in the AdAQP1 clinical trial. On the other hand, the absence or alternate isoforms of major salivary proteins such as Amylase, Lactoferrin and Lactoperoxidase (Table 2) makes it likely that the fluid produced may lack the efficacy of natural saliva in preventing caries and preserving the overall health of the oral mucosa. Finally, perhaps the most clinically relevant observation made in this study is the ability of AQP1 gene therapy delivered to the irradiated parotid gland to restore and even augment the function of the contralateral, undamaged gland. Integrating area-under-the-curve in Figure 6, it appears that the majority of the saliva produced as a result of our UAGT/AQP1 gene therapy intervention actually came from the undamaged parotid gland, and if this principle holds true in human patients, the benefit to the maintenance of oral and dental health is likely to be very significant.

This study has several limitations that should be noted, and are imposed either due to logistical challenges with this large animal model or economy of animal use for experimental design. First, the 10Gy radiation is a mild insult, and is delivered as a single dose, in contrast to the fractionated dosing used clinically. As noted in Methods, a 20Gy electron beam causes severe radiation burns, and our ongoing experiments suggest that 15Gy may be suitable for future studies. Second, we have not shown immunohistochemical localization of pAQP1 expression in our treated minipigs, although we have previously shown immunohistochemical distribution of a transgene in the salivary glands of mice following UAGT(9) and expect a similar pattern in minipigs.

With it now possible that UAGT can replace Adenovirus as the gene transfer technology to carry forward as a gene therapy for radiation-induced xerostomia, it is important to consider the state of the art vis-à-vis the plasmid vector. Conventional plasmid vectors contain extensive backbone regions of bacterial origin, and these regions are thought to stimulate host immunity and transgene silencing through various mechanisms that are as yet incompletely characterized (9, 32–36). Minimalist plasmid constructs, termed “minicircles” or “mini-intronic plasmids” delete all or most of the foreign backbone sequences, but are more difficult and costly to manufacture than conventional plasmids, particularly at the microgram quantities required for our application. Nevertheless, work from our own group has shown minicircles to be superior vectors for UAGT to the salivary gland (9). Our gene therapy strategy, as well as others in the preclinical pipeline, would likely benefit from technological advancement allowing for GMP production of minicircles in the microgram range, at reasonable cost. Finally, UAGT is theoretically suitable for the delivery of gene editing components (e.g. CRISPR/Cas) to the salivary gland, and the potential for this emerging technology as a means of permanent insertion of AQP1into surviving ductal cells should be considered in future studies.

Methods

Animals and husbandry

The Institutional Animal Care and Use Committee of Allegheny Singer Research Institute approved all animal experimentation described herein. Yucatan miniature swine aged approximately 10 weeks were purchased from Sinclair BioResources (Columbia, MO, USA). This well-characterized colony is certified free of common swine diseases and is vaccinated for *Haemophilus*, *erysipelas*, PCV and *mycoplasma*.

Animals were group housed in large pens, with temperature maintained at 21–26° C and 30–70% humidity under positive pressure. Enrichment with toys and human contact was provided. Subjects were fed twice daily, according to the breeder's recommendations and allowed free access to water via an automatic system. Subjects acclimated to our colony for one week before being entered into the study. Experimental group assignments are outlined in Figure 1. Group sizes were based upon pilot studies indicating that n=4 gave a significant effect in gene therapy-treated animals. Animals received a name designation and were randomly assigned to their experimental group upon receipt in our facility.

Electron beam treatment planning and irradiation

Earlier studies (data not shown) utilizing a 20Gy electron beam revealed extremely severe damage to the parotid gland, well in excess of that experienced by most patients suffering from radiation-induced xerostomia. We calculated a single 10Gy dose of electrons to be approximately bioequivalent to the threshold dose for parotid gland dysfunction. The functional deficits reported in Figure 2C validate this mild dose of radiation as being sufficient to elicit profound functional deficits in the parotid glands of our swine subjects.

A treatment plan was devised by computerized tomographic scanning of a single minipig of similar size and weight to all others in the study. This animal subject was used as a model for a vacuum formed bag to ensure targeting accuracy and immobilization of all subjects. This vacuum formed bag was subsequently used for immobilization of all animals participating in the study. CT scanning of this animal was performed using a Siemens Somatom Sensation® scanner (Concord, CA, USA), and radiation treatment planning was performed on a Computerized Medical Systems XIO® (Maryland Heights, MO, USA) planning system. A DRR image of the treatment plan is presented in Figure 2A, showing the anatomical location of the left and right parotid glands in relationship to the mandible and to one another.

Based upon this treatment plan, irradiation of the right parotid gland was performed in all animal subjects using a Siemens Primus® (Concord, California) linear accelerator. Animals were sedated and placed in the vacuum form bag in the linear accelerator. A 12 MeV electron beam calculated at the 90% isodose line was used to treat the gland, exempting a small portion of the anteromedial region to avoid unintended irradiation of the contralateral gland due to the anatomic proximity of the two structures in this area. Cerrobend® (Bolton Metal Products, Bellefonte, Pa), an eutectic alloy comprised of 50% bismuth, 26.7% lead, 13.3% tin, and 10% cadmium by weight was used to block the electron beam from surrounding structures following custom anatomic fitting to match the right swine parotid

gland. A 1.0 cm margin around the target gland was added to the aperture of the block to allow for respiratory motion and to allow build-up of electron dose. Following irradiation and recovery from sedation, all animals were returned to the husbandry unit without event.

Saliva collection

All saliva collections were performed between 6:30am and 10:00am, and the timepoints of saliva collection are shown in the respective figures. No blinding was utilized in this study. Animals were initially sedated by intramuscular injection of a mixture of ketamine (20mg/kg) and xylazine (2mg/kg), then placed on an operating table, intubated, and place in the prone position, maintained with isoflurane anesthesia (1–1.5%) via artificial ventilation. An intramuscular injection of 1mg/kg of Pilocarpine was given and 10–15 minutes were allowed to elapse for the sialogogue to take effect (determined by pooling of saliva in the anterior floor of the mouth). An oral swab with a 2mL capacity (Salimetrics, Carlsbad, CA, USA) was weighed and then placed over the opening of Stensen's duct, in the buccal corridor and mechanically secured. Saliva was collected by capillary action for 10 minutes, and the oral swab was replaced if it appeared to be approaching capacity. After 10 minutes, the oral swab(s) were weighed and saliva volume calculated by subtracting initial weight from final weight, assuming a specific gravity of 1 for the saliva. Saliva was removed from the oral swab by centrifugation at 3000rpm for 15 minutes at 4C and analyzed as described.

pAQP1 construction and testing

Porcine (*Sus scrofa)* AQP1 (NCBI, NM_414454) was synthesized by Integrated DNA Technologies (Coralville, IA, USA). The cDNA was amplified with the following primers: Forward: 5′-ATAGGATCCACCTGGCCAGCGAGTTCAAGAAGAAG, Reverse 5′-TATCTCGAG TTATTTGGGCTTCATCTCCAC and cloned into pCMV-MCS (Agilent Technologies, Santa Clara, CA, USA) using *BamHI* and *XhoI* restriction sites, resulting in pCVM-pAQP1.

pAQP1 channel function was tested by expressing the pCMV-pAQP1 plasmid in Madin-Darby Canine Kidney epithelial (MDCK) cells (Source: ATCC). Transfection was performed using Lipofectamine 2000 (Life Technologies, Carlsbad, CA, USA), using a GFP-expressing plasmid in parallel cultures as a control for transfection efficiency. 48 hours after transfection, cells were seeded on collagen-coated polycarbonate filter inserts in six-well plates (Corning, Corning, NY, USA) and placed in a transwell system as shown in Figure 5A. After cells formed a confluent monolayer, the apical chamber was replaced with 1.5 ml hyperosmotic sucrose/DMEM medium (440 mOsmol/L) and the medium in the basal chamber was replaced with fresh 2.6ml DMEM medium. After 48hr, the fluid volume in the individual apical chambers was measured by pipette and the transepithelial net fluid movement was calculated relative to GFP controls.

Adenoviral vector construction, purification, and testing

The AdhAQP1, obtained as an aliquot of the clinically-validated vector, provided as a kind gift from Dr. Changyu Zhang (NIDCR). This vector was not further tested prior to upscaling. The vector was upscaled in HEK293 cell cultures, and purified using 2X CsCl gradient centrifugation. Viral titer (vp) was determined using optical absorbance.

In order to construct a recombinant adenovirus encoding porcine AQP1, the pAQP1 cDNA was amplified from pCMV-pAQP1, described above, using the following primers: Forward: 5′-GCTCGAGCCTAAG TTCCACCATGGCCA CGAGTCAGGAAG, Reverse 5′-TCTTATCTAGAAGCTTTTATTTGGGCTTCATCT CCAC. The cDNA was cloned into the HindIII restriction site of the pShuttle-CMV vector (Agilent Technologies, Carlsbad, CA, USA) using the In-Fusion cloning system (Clontech, Mountain View, CA, USA). The resulting pShuttle-pAQP1 was linearized by digestion with PmeI and transformed into *E.coli* BJ 5183-AD-1 strain cells (Agilent Technologies). Recombinant clones was selected by kanamycin resistance and confirmed by *PacI* endonuclease restriction analysis. Finally the linearized recombinant plasmid was transfected into HEK293 cells by Polyethylenimine transfection. The primary viral stock was prepared by freeze/thaw cycles of cells 15 days post-transfection. The AdpAQP1 was upscaled and purified as described above and functionally tested using the transwell system described for the pCMV-pAQP1 plasmid.

Gene transfer to the salivary gland

All gene transfer procedures were performed between 6:30am and 10:00am. The animals were sedated, intubated, and positioned as described under Saliva Collection above, with the exception that animals are placed supine for cannulation of Stensen's duct. An intramuscular injection of 0.54mg atropine was given and 10 minutes were allowed to elapse for the drug to take effect. A P50 catheter fused to a P10 catheter was inserted into the opening of Stensen's duct on the right side and secured with Vetbond (3M Products, St. Paul, MN, USA). All infusions were made using 3 ml of sterile phosphate-buffered saline and the tubing left in place for 10 minutes following infusion. For Adenoviral gene delivery, 1×10^{10} viral particles of AdhAQP1 or AdpAQP1 were diluted in the infusate. All gene transfer studies were carried out on the right parotid gland only, and the left (control) gland was never cannulated.

For UAGT, Definity microbubbles (Lantheus Medical Imaging, North Billerica, MA) were activated per manufacturer's instructions immediately prior to the procedure and mixed with 1mg/ml of the plasmid vector (either pCMV-pAQP1 or pCMV-MetLuc) before being added to the infusate (total dose 3mg). Immediately after infusion, a layer of clinical ultrasound gel was applied to the skin overlying the parotid gland and SoniGene ultrasound beam emitter (VisualSonics, Toronto, Canada) was applied to the skin and moved over the outline of the parotid gland using a gliding motion. A total ultrasound exposure of 4 treatments comprising 30 seconds each, $2W/cm^2$ at a 50% duty cycle with 10 seconds between treatments was delivered. Following gene transfer, the animal was allowed to awaken and returned to its housing.

Tissue processing and histological analysis

Parotid glands were dissected from the specimen, partially section across the transverse plane (i.e. "bread loafed") to facilitate fixation, and immediately fixed in 20 volumes of formalin per weight. The glands were examined and at least 5 representative sections were harvested per each gland. Tissue sections were processed for conventional H&E staining.

Statistical analysis

For statistical comparisons of measurements at a single timepoint, including Figure 2B, 3A, and 5B, an unpaired, single-tailed t-test was utilized. For statistical comparisons of multiple saliva measurements made over time, including Figure 2C, 3B, 4, and 6, a repeated Measures ANOVA with mixed effects using a compound symmetry variance and post-hoc Tukey adjusted differences of least squares mean was utilized. In all analyses, p values of <0.05 were considered significant.

Proteomic profiling of swine saliva

Proteomic profiling was performed on pig saliva using methods similar to those we have previously described (9). Briefly, a clean-up step was performed using a 2-D Quant kit (GE Healthcare, Little Chalfont, Buckinghamshire, UK) and dissolved using 2D gel rehydration buffer with 50 mM Tris pH8.5. Protein concentrations were evaluated using Bradford method and samples were appropriate diluted to a final protein concentration of 1μg/μl. 1μl of Cy3 or Cy5 NHS-conjugated dyes (Lumiprobe, Inc., Hallandale Beach, FL, USA) were added to 50 μg of protein sample and incubated on ice for 30 min in the dark. 1μl of 10 mM lysine was used to quench the reaction by incubating on ice for 10 min in the dark.

2-D SDS gels were run mixing 10μg of each paired sample and diluting further in rehydration buffer to 450μl and placing on a 24 cm IEF strip (pH3-10NL). These strips were previously rehydrated using 2% DTT, 0.5% IPG buffer and 0.002% bromophenol blue at RT for 8 hours. Rehydrated strips were loaded on Ettan IPGphor 3 IEF system, samples were placed, and run overnight for a total of 60,000 volt-hours (vhr) and equilibrated with 1% DTT followed by 2.5% iodoacetamide for 15 min each. The second dimension was carried out in a homogeneous 13.5% SDS gel.

Completed gels were scanned using a Typhoon 9400 scanner. The pictures were edited using ImageQuant TL 7.0 software and Differential In-gel Analysis (DIA) and Biological Variation Analysis (BVA) of the 2D DiGE results were performed using DeCyder 2D 7.0 Software (GE Healthcare). All protein spots-of-interest, identified by BVA and DIA analyses, were manually checked to insure that they were not changed in the Baseline versus Control gels, and thus the decrease or loss of these proteins can be definitively attributed to the effects of irradiation and/or gene therapy. Spots identified as being significantly decreased in the Baseline versus UAGT/pAQP1 gels but unchanged in the Baseline versus Control gels were extracted using an Ettan Spot Picker (GE Healthcare).

Protein identification was performed as previously described (37). Briefly, protein spots of interest from 2D gels were excised, reduced with DTT and alkylated with iodoacetamide, digested with trypsin and desalted with C18 ZipTips (Millipore, Billerica, MA, USA). Both MS and MS/MS analyses of the digested peptides were performed on a MALDI-TOF/TOF tandem MS (Bruker UltrafleXtreme, Bruker Daltonics Inc. Billerica, MA, USA). The database search and analysis were performed using FlexAnalysis and BioTools software (Bruker Daltonics Inc.) against “Other Mammalia (excluding primate and rodents) Swiss-Prot protein database using a local Mascot server.

Acknowledgments

These studies were supported by NIH grant #DE022973 (to MJP). The authors wish to thank E. Day Werts, PhD for expert assistance in designing the irradiation protocol. The authors also gratefully acknowledge the assistance of Suzanne Ezzo, Tara Fraser, and Ashley Wilferd with animal procedures, Carol Bain for assistance with preparation of histological specimens and Kelly Shields, PhD for assistance with statistical analyses.

References

1. Jemal A, Siegel R, Xu J, Ward E. Cancer statistics, 2010. CA Cancer J Clin. 2010 Sep-Oct;60(5): 277–300. [PubMed: 20610543]
2. NCI Statistics. Available from: http://www.cancer.gov/statistics
3. Chera BS, Eisbruch A, Murphy BA, Ridge JA, Gavin P, Reeve BB, et al. Recommended patient-reported core set of symptoms to measure in head and neck cancer treatment trials. J Natl Cancer Inst. 2014 Jul.106(7)
4. Baum BJ, Alevizos I, Zheng C, Cotrim AP, Liu S, McCullagh L, et al. Early responses to adenoviral-mediated transfer of the aquaporin-1 cDNA for radiation-induced salivary hypofunction. Proc Natl Acad Sci U S A. 2012 Nov 20; 109(47):19403–7. [PubMed: 23129637]
5. Baum BJ, Zheng C, Cotrim AP, Goldsmith CM, Atkinson JC, Brahim JS, et al. Transfer of the AQP1 cDNA for the correction of radiation-induced salivary hypofunction. Biochim Biophys Acta. 2006 Aug; 1758(8):1071–7. Epub 2005/12/22. eng. [PubMed: 16368071]
6. Morral N, O'Neal W, Rice K, Leland M, Kaplan J, Piedra PA, et al. Administration of helper-dependent adenoviral vectors and sequential delivery of different vector serotype for long-term liver-directed gene transfer in baboons. Proc Natl Acad Sci U S A. 1999 Oct 26; 96(22):12816–21. [PubMed: 10536005]
7. Fontanellas A, Hervas-Stubbs S, Mauleon I, Dubrot J, Mancheno U, Collantes M, et al. Intensive pharmacological immunosuppression allows for repetitive liver gene transfer with recombinant adenovirus in nonhuman primates. Mol Ther. 2010 Apr; 18(4):754–65. [PubMed: 20087317]
8. Passineau MJ, Zourelias L, Machen L, Edwards PC, Benza RL. Ultrasound-assisted non-viral gene transfer to the salivary glands. Gene Ther. 2010 Nov; 17(11):1318–24. Epub 2010/05/29. eng. [PubMed: 20508599]
9. Geguchadze R, Wang Z, Zourelias L, Perez-Riveros P, Edwards P, Machen L, et al. Proteomic profiling of salivary gland after non-viral gene transfer mediated by conventional plasmids and minicircles. Molecular Therapy - Methods and Clinical Development. 2014 Apr 2.2014
10. Definity Package Insert. Available from: http://www.definityimaging.com/pdf/DEFINITYPrescribingInformation515987-0413.pdf
11. Baum BJ, Zheng C, Alevizos I, Cotrim AP, Liu S, McCullagh L, et al. Development of a gene transfer-based treatment for radiation-induced salivary hypofunction. Oral Oncol. 2010 Jan; 46(1): 4–8. [PubMed: 19892587]
12. Markova SV, Golz S, Frank LA, Kalthof B, Vysotski ES. Cloning and expression of cDNA for a luciferase from the marine copepod Metridia longa. A novel secreted bioluminescent reporter enzyme. J Biol Chem. 2004 Jan 30; 279(5):3212–7. [PubMed: 14583604]
13. Delporte C, O'Connell BC, He X, Lancaster HE, O'Connell AC, Agre P, et al. Increased fluid secretion after adenoviral-mediated transfer of the aquaporin-1 cDNA to irradiated rat salivary glands. Proc Natl Acad Sci U S A. 1997 Apr 1; 94(7):3268–73. [PubMed: 9096382]
14. Shan Z, Li J, Zheng C, Liu X, Fan Z, Zhang C, et al. Increased fluid secretion after adenoviral-mediated transfer of the human aquaporin-1 cDNA to irradiated miniature pig parotid glands. Mol Ther. 2005 Mar; 11(3):444–51. Epub 2005/02/25. eng. [PubMed: 15727941]
15. Elmore S, Lanning L, Allison N, Vallant M, Nyska A. The transduction of rat submandibular glands by an adenoviral vector carrying the human growth hormone gene is associated with limited and reversible changes at the infusion site. Toxicol Pathol. 2006; 34(4):385–92. [PubMed: 16844666]
16. Zheng C, Voutetakis A, Kok MR, Goldsmith CM, Smith GB, Elmore S, et al. Toxicity and biodistribution of a first-generation recombinant adenoviral vector, in the presence of

hydroxychloroquine, following retroductal delivery to a single rat submandibular gland. Oral Dis. 2006 Mar; 12(2):137–44. [PubMed: 16476034]

17. Delporte C, Miller G, Kagami H, Lillibridge CD, O'Connell BC, Atkinson JC, et al. Safety of salivary gland-administered replication-deficient recombinant adenovirus in rats. J Oral Pathol Med. 1998 Jan; 27(1):34–8. [PubMed: 9466733]
18. Adesanya MR, Redman RS, Baum BJ, O'Connell BC. Immediate inflammatory responses to adenovirus-mediated gene transfer in rat salivary glands. Hum Gene Ther. 1996 Jun 10; 7(9): 1085–93. [PubMed: 8773510]
19. Zheng C, Goldsmith CM, Mineshiba F, Chiorini JA, Kerr A, Wenk ML, et al. Toxicity and biodistribution of a first-generation recombinant adenoviral vector, encoding aquaporin-1, after retroductal delivery to a single rat submandibular gland. Hum Gene Ther. 2006 Nov; 17(11):1122–33. [PubMed: 17069536]
20. Delporte C. Role of aquaporins in saliva secretion. OA Biochemistry. 2013 Sep 01.1(2)
21. Wong DT. Salivaomics. J Am Dent Assoc. 2012 Oct; 143(10 Suppl):19S–24S. [PubMed: 23034834]
22. Mastrangeli A, O'Connell B, Aladib W, Fox PC, Baum BJ, Crystal RG. Direct in vivo adenovirus-mediated gene transfer to salivary glands. Am J Physiol. 1994 Jun; 266(6 Pt 1):G1146–55. [PubMed: 8023944]
23. Vissink A, Mitchell JB, Baum BJ, Limesand KH, Jensen SB, Fox PC, et al. Clinical management of salivary gland hypofunction and xerostomia in head-and-neck cancer patients: successes and barriers. Int J Radiat Oncol Biol Phys. 2010 Nov 15; 78(4):983–91. [PubMed: 20970030]
24. Li J, Shan Z, Ou G, Liu X, Zhang C, Baum BJ, et al. Structural and functional characteristics of irradiation damage to parotid glands in the miniature pig. Int J Radiat Oncol Biol Phys. 2005 Aug 1; 62(5):1510–6. [PubMed: 16029813]
25. Suwabe T, Fukami H, Bradley RM. Synaptic responses of neurons controlling the parotid and von Ebner salivary glands in rats to stimulation of the solitary nucleus and tract. Journal of neurophysiology. 2008 Mar; 99(3):1267–73. [PubMed: 18199816]
26. Kasarskis EJ, Hodskins J, St Clair WH. Unilateral parotid electron beam radiotherapy as palliative treatment for sialorrhea in amyotrophic lateral sclerosis. Journal of the neurological sciences. 2011 Sep 15; 308(1–2):155–7. [PubMed: 21726879]
27. Unzu C, Hervas-Stubbs S, Sampedro A, Mauleon I, Mancheno U, Alfaro C, et al. Transient and intensive pharmacological immunosuppression fails to improve AAV-based liver gene transfer in non-human primates. Journal of translational medicine. 2012; 10:122. [PubMed: 22704060]
28. McIntosh JH, Cochrane M, Cobbold S, Waldmann H, Nathwani SA, Davidoff AM, et al. Successful attenuation of humoral immunity to viral capsid and transgenic protein following AAV-mediated gene transfer with a non-depleting CD4 antibody and cyclosporine. Gene Ther. 2012 Jan; 19(1):78–85. [PubMed: 21716299]
29. Flotte TR. Recent developments in recombinant AAV-mediated gene therapy for lung diseases. Curr Gene Ther. 2005 Jun; 5(3):361–6. [PubMed: 15975013]
30. Kok MR, Voutetakis A, Yamano S, Wang J, Cotrim A, Katano H, et al. Immune responses following salivary gland administration of recombinant adeno-associated virus serotype 2 vectors. J Gene Med. 2005 Apr; 7(4):432–41. [PubMed: 15515118]
31. Loo JA, Yan W, Ramachandran P, Wong DT. Comparative human salivary and plasma proteomes. J Dent Res. 2010 Oct; 89(10):1016–23. [PubMed: 20739693]
32. Gracey Maniar LE, Maniar JM, Chen ZY, Lu J, Fire AZ, Kay MA. Minicircle DNA vectors achieve sustained expression reflected by active chromatin and transcriptional level. Mol Ther. 2013 Jan; 21(1):131–8. [PubMed: 23183534]
33. Lu J, Zhang F, Kay MA. A mini-intronic plasmid (MIP): a novel robust transgene expression vector in vivo and in vitro. Mol Ther. 2013 May; 21(5):954–63. [PubMed: 23459514]
34. Chen ZY, Riu E, He CY, Xu H, Kay MA. Silencing of episomal transgene expression in liver by plasmid bacterial backbone DNA is independent of CpG methylation. Mol Ther. 2008 Mar; 16(3): 548–56. [PubMed: 18253155]

35. Nakai H, Yant SR, Storm TA, Fuess S, Meuse L, Kay MA. Extrachromosomal recombinant adeno-associated virus vector genomes are primarily responsible for stable liver transduction in vivo. J Virol. 2001 Aug; 75(15):6969–76. [PubMed: 11435577]

36. Lu J, Zhang F, Xu S, Fire AZ, Kay MA. The extragenic spacer length between the 5′ and 3′ ends of the transgene expression cassette affects transgene silencing from plasmid-based vectors. Mol Ther. 2012 Nov; 20(11):2111–9. [PubMed: 22565847]

37. Wu C, Liu T, Chen W, Oka S, Fu C, Jain MR, et al. Redox regulatory mechanism of transnitrosylation by thioredoxin. Molecular & cellular proteomics : MCP. 2010 Oct; 9(10):2262–75. [PubMed: 20660346]

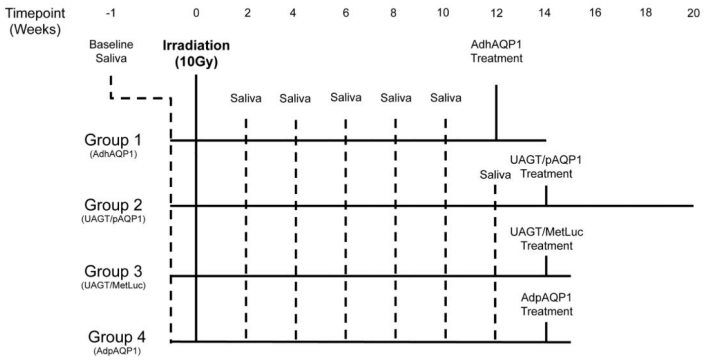

Group #	Treatment	n	Treatment Timepoint (Weeks Post-Irradiation)	Survival Post-Treatment (Weeks)	Comments	Post-Treatment Saliva Measurements
1	AdhAQP1 (NIH virus)	4	12	2	Model Validation	Figure 4
2	UAGT/pAQP1	4	14	6	Experimental	Figure 6
3	UAGT/MetLuc	4	14	1	Negative Control, Histology	Figure 3B
4	AdpAQP1	4	14	1	Histology Only	-

Figure 1.

Experimental group assignments for the 16 animal subjects participating in this study.

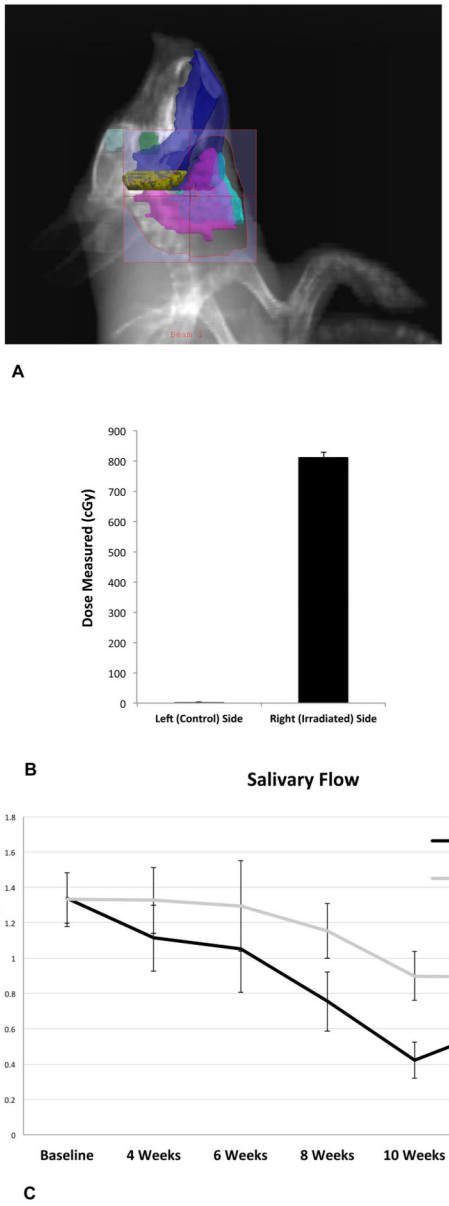

Figure 2. Radiation treatment plan, dosimetry study, and radiation-induced hyposalivation

(A) Digital radiography reconstruction of the head of a Yucatan minipig utilized in this study. The right parotid gland, the target organ for irradiation, is shown in magenta. Other structures important to the treatment plan include left parotid (indigo), mandible (dark blue/yellow), right orbit (cyan) and left orbit (dark green). (B) Radiation dose measured on the skin overlying the left (control) and right (irradiated) parotid glands. (C) Stimulated isolated parotid saliva volumes at pre-irradiation baseline and various time points post-irradiation in the 16 subjects participating in this study. Error bars are +/− SEM. Statistical analysis determined that significant differences exsited between irradiated and control volumes (p=0.0003) but no interaction beween the covariates suggesting both groups changing over time at similar rates. Evaluating the treatment status versus baseline across all weeks

indicated that the irradiated side was significantly different than baseline (p=0.0002) but the control side was not (p=0.5).

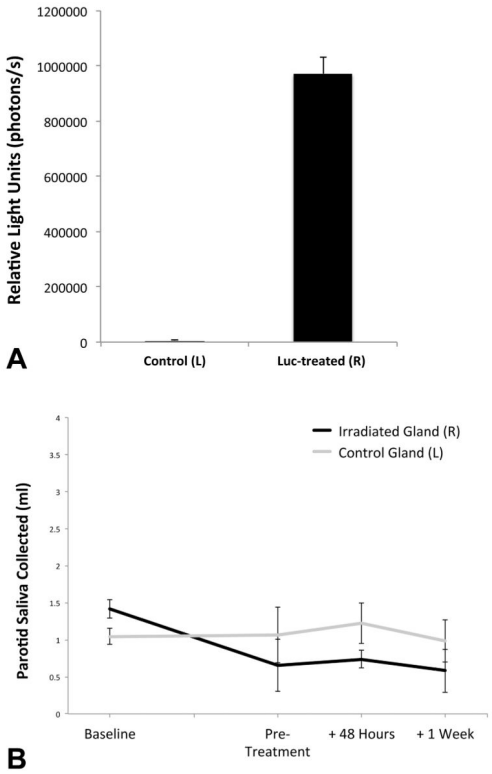

Figure 3. Ultrasound-assisted non-viral gene transfer to the parotid gland of Yucatan minipig

(A) Relative light units (photons/s) measured from stimulated saliva samples taken 48 hours following UAGT of a MetLuc-expressing plasmid to the right (R) parotid gland (n=4). The difference between luminescence of saliva from right and left (L) was highly significant ($p<0.01$). (B) Stimulated parotid saliva volumes at Baseline, Pre-Treatment, and 48 hours and 1 week following UAGT of MetLuc. Error bars are +/− SEM.

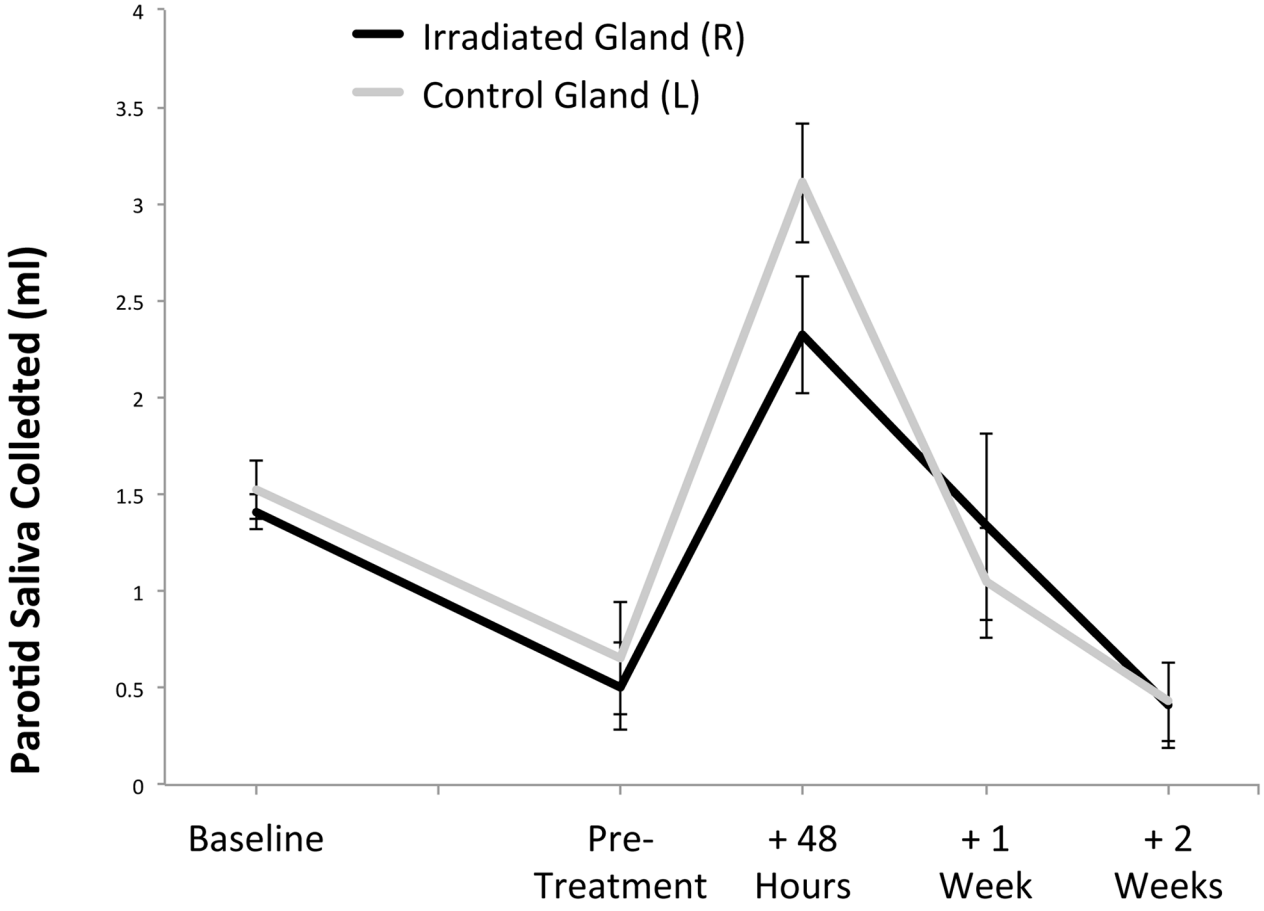

Figure 4. AdhAQP1 gene therapy in our swine model of radiation-induced hyposalivation

Stimulated parotid saliva volumes at Baseline, Pre-Treatment (12 weeks post-irradiation), and 48 hours and 1 week and 2 weeks following gene therapy with 1×10^{10}vp of AdhAQP1 (n=4). Error bars are +/− SEM. Statistical analysis determined that no significant differences existed between irradiated (R) and control (L) gland saliva volumes (p=0.4) suggesting both groups change together. Comparisons between weeks noted the following significant differences: Baseline versus Pretreatment (p=0.01), Pretreatment versus +48 Hours (0.0001), +48 Hours versus +1 Week (p=0.0001).

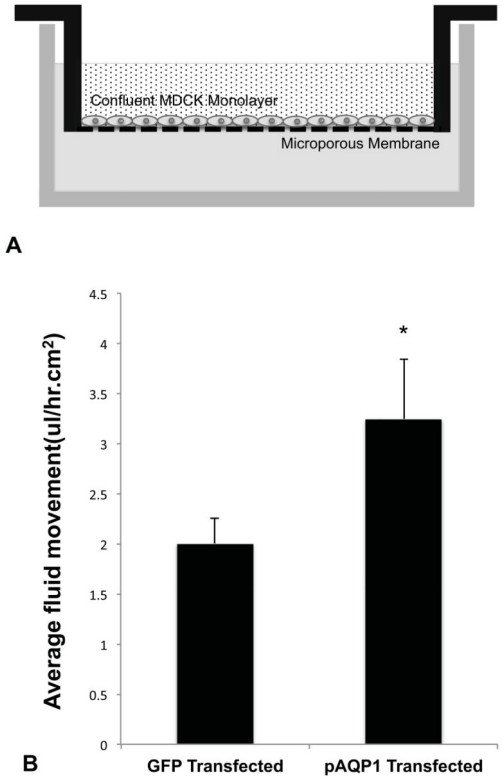

Figure 5. Testing of pAQP1 channel function

(A) Schematic of the transwell culture system utilized to assess transcellular fluid flux across a confluent MDCK monolayer. The upper layer of the well is 440mOsmol/L hyperosmotic sucrose/DMEM media and the lower layer is standard DMEM media. (B) Quantification of transcellular flux in GFP-transfected and pAQP1-transfected MDCK cells over a 48 hour period. * indicates statistically significant ($p<0.05$) difference between GFP- and pAQP1-transfected cells. Error bars are +/− SEM.

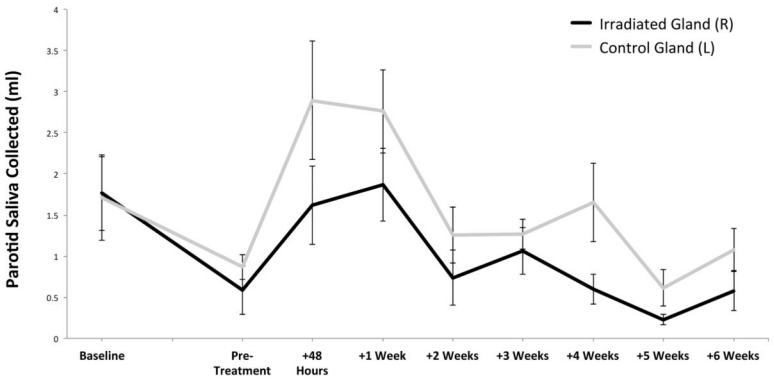

Figure 6. pAQP1 gene therapy using UAGT in our irradiated pig model

Stimulated parotid saliva volumes at Baseline, Pre-Treatment (14 weeks post-irradiation), and 48 hours, 1 week, 2 weeks, 3 weeks, 4 weeks, 5 weeks and 6 weeks following gene therapy with UAGT/pCMV-AQP1 (n=4). Error bars are +/− SEM. Statistical analysis determined that no significant differences exsited between irradiated and control volumes (p=0.0009) but no interaction beween the covariates suggesting both groups changing over time at similar rates. Comparisons between weeks noted the following significant differences: Baseline versus Pretreatment (p=0.06), Pretreatment versus +48 Hours (0.06), +48 Hours versus +1 Week (p=0.004).

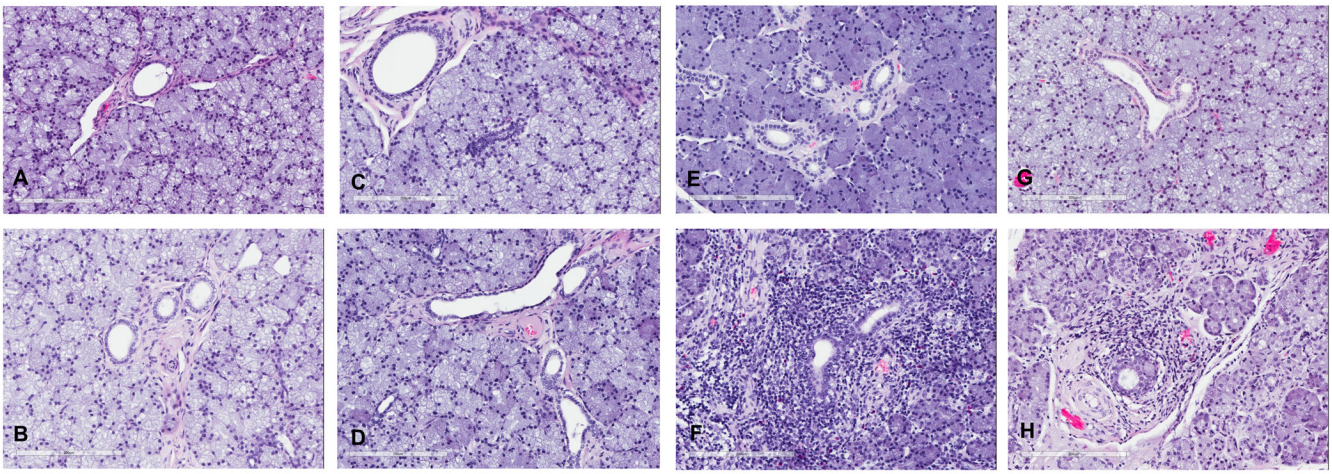

Figure 7. Representative histology of parotid glands 1 week following Adenoviral gene transfer and UAGT

The top row (A, C, E, G) are contralateral, non-irradiated control glands from the corresponding treated animals in the bottom row (B, D, F, H). B and D are UAGT/pAQP1-treated and F and H are AdpAQP1 treated. Scale bars are 200μm.

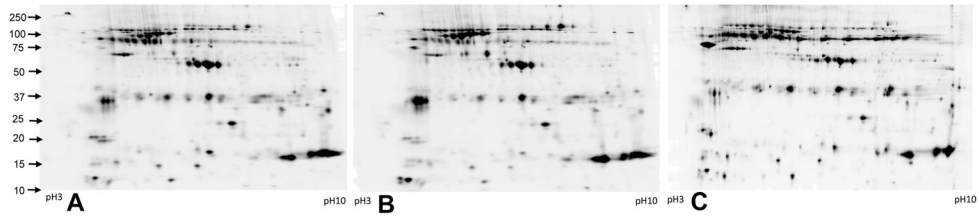

Figure 8. Proteomic profiling of pooled saliva obtained from and pre-injury baseline (A), contralateral control glands (B) and irradiated, UAGT/pAQP1-treated parotid glands (n=4/ group) 2 weeks after UAGT treatment

Each image is a grayscale representation of fluorescent intensity of a pooled sample of each group, each labeled with a different Cy dye (Cy2, Cy3, Cy5). Pooled samples were run simultaneously on the same gel, and groups were differentiated by their Cy dye and images corrected to compensate for differences in dye fluorescence intensity. These profiles are generated for visual purposes and were not utilized for statistical analysis.

Gene Ther. Author manuscript; available in PMC 2016 March 01.

Table 1

Blinded expert histological analysis of parotid glands 1 week following Adenoviral gene transfer and UAGT.

Animal #		Side	Treatment	Glandular Acini	Glandular Interstitium
9	Group 3	R	Irradiation, UAGT/MetLuc	Swelling, vacuolization, zymogen granule pleomorphism	Minimal periductal lymphocytic infiltration
		L	None	Normal	Normal
10		R	Irradiation, UAGT/MetLuc	Swelling, vacuolization, zymogen granule pleomorphism	Normal
		L	None	Normal	Normal
11		R	Irradiation, UAGT/MetLuc	Swelling, vacuolization, zymogen granule pleomorphism	Normal
		L	None	Normal	Normal
12		R	Irradiation, UAGT/MetLuc	Swelling, vacuolization, zymogen granule pleomorphism	Normal
		L	None	Normal	Normal
13	Group 4	R	Irradiation, AdpAQP1	Swelling, vacuolization, zymogen granule pleomorphism	Moderate periductal fibrosis, moderate periductal lymphocytic infiltration, salivary ductal ectasia
		L	None	Normal	Normal
14		R	Irradiation, AdpAQP1	Swelling, vacuolization, zymogen granule pleomorphism	Moderate periductal fibrosis, moderate periductal lymphocytic infiltration, perivascular sclerosis
		L	None	Normal	Normal
15		R	Irradiation, AdpAQP1	Swelling, vacuolization, zymogen granule pleomorphism, focal atrophy	Mild periductal fibrosis, moderate periductal lymphocytic infiltration
		L	None	Normal	Normal
16		R	Irradiation, AdpAQP1	Swelling, vacuolization, zymogen granule pleomorphism	Normal
		L	None	Normal	Normal

Table 2

Identities of proteins determined to be significantly reduced in saliva obtained from irradiated, UAGT/pAQP1-treated parotid glands relative to saliva obtained at the same time from contralateral, control glands. Data a separated according to their database identification, either from the swine database, or the other mammals database.

Accession #	Description	Fold-Change (AQP1-treated/Baseline)
Pig Database		
CP8B1_PIG	5-beta-cholestane-3-alpha,7-alpha-diol 12-alpha-hydroxylase OS=Sus scrofa GN=CYP8B1 PE=2 SV=1	−2.2
5HT1D_PIG	5-hydroxytryptamine receptor 1D (Fragment) OS=Sus scrofa GN=HTR1D PE=2 SV=1	−2.5
ACTS_PIG	Actin, alpha skeletal muscle OS=Sus scrofa GN=ACTA1 PE=3 SV=1	2.2
ACTB_PIG	Actin, cytoplasmic 1 OS=Sus scrofa GN=ACTB PE=2 SV=2	2.2
ADML_PIG	ADM OS=Sus scrofa GN=ADM PE=1 SV=1	2.0
ATPD_PIG	ATP synthase subunit delta, mitochondrial (Fragment) OS=Sus scrofa GN=ATP5D PE=2 SV=1	3.4
CAN1_PIG	Calpain-1 catalytic subunit OS=Sus scrofa GN=CAPN1 PE=2 SV=3	2.2
CHLE_PIG	Cholinesterase (Fragment) OS=Sus scrofa GN=BCHE PE=2 SV=1	−6.1
CO3_PIG	Complement C3 OS=Sus scrofa GN=C3 PE=1 SV=2	2.9
CP2E1_PIG	Cytochrome P450 2E1 OS=Sus scrofa GN=CYP2E1 PE=2 SV=1	2.1
HPT_PIG	Haptoglobin OS=Sus scrofa GN=HP PE=1 SV=1	2.5
LAC_PIG	Ig lambda chain C region OS=Sus scrofa PE=1 SV=1	3.3
MOES_PIG	Moesin OS=Sus scrofa GN=MSN PE=2 SV=3	2.7
MYH1_PIG	Myosin-1 OS=Sus scrofa GN=MYH1 PE=2 SV=1	2.4
OPTN_PIG	Optineurin OS=Sus scrofa GN=OPTN PE=1 SV=1	2.5
AMYP_PIG	Pancreatic alpha-amylase OS=Sus scrofa GN=AMY2 PE=1 SV=3	2.9
PECA1_PIG	Platelet endothelial cell adhesion molecule OS=Sus scrofa GN=PECAM1 PE=2 SV=1	2.2
COLI_PIG	Pro-opiomelanocortin OS=Sus scrofa GN=POMC PE=1 SV=1	2.0
S10AC_PIG	Protein S100-A12 OS=Sus scrofa GN=S100A12 PE=1 SV=2	3.5
SAL_PIG	Salivary lipocalin OS=Sus scrofa GN=SAL1 PE=1 SV=1	6.7
TRFE_PIG	Serotransferrin OS=Sus scrofa GN=TF PE=1 SV=2	−3.3
ALBU_PIG	Serum albumin OS=Sus scrofa GN=ALB PE=1 SV=2	2.1
SDHB_PIG	Succinate dehydrogenase [ubiquinone] iron-sulfur subunit, mitochondrial OS=Sus scrofa GN=SDHB PE=1 SV=1	2.0
TPM4_PIG	Tropomyosin alpha-4 chain OS=Sus scrofa GN=TPM4 PE=2 SV=3	4.5
TRYP_PIG	Trypsin OS=Sus scrofa PE=1 SV=1	2.3
MYO7A_PIG	Unconventional myosin-VIIa (Fragment) OS=Sus scrofa GN=MYO7A PE=2 SV=1	3.4

Accession #	Description	Fold-Change (AQP1-treated/Baseline)
UPK2_PIG	Uroplakin-2 OS=Sus scrofa GN=UPK2 PE=2 SV=3	−6.0
Other Mammalian Database (excluding Primates and Rodents)		
1433B_BOVIN	14-3-3 protein beta/alpha OS=Bos taurus GN=YWHAB PE=1 SV=2	5.5
1433E_BOVIN	14-3-3 protein epsilon OS=Bos taurus GN=YWHAE PE=2 SV=1	5.5
1433F_BOVIN	14-3-3 protein eta OS=Bos taurus GN=YWHAH PE=1 SV=2	5.5
1433G_BOVIN	14-3-3 protein gamma OS=Bos taurus GN=YWHAG PE=1 SV=2	5.5
1433S_BOVIN	14-3-3 protein sigma OS=Bos taurus GN=SFN PE=2 SV=1	5.5
1433T_BOVIN	14-3-3 protein theta OS=Bos taurus GN=YWHAQ PE=2 SV=1	5.5
1433Z_BOVIN	14-3-3 protein zeta/delta OS=Bos taurus GN=YWHAZ PE=1 SV=1	5.5
ACTC_BOVIN	Actin, alpha cardiac muscle 1 OS=Bos taurus GN=ACTC1 PE=2 SV=1	2.2
ACTA_BOVIN	Actin, aortic smooth muscle OS=Bos taurus GN=ACTA2 PE=1 SV=1	2.2
ACTH_BOVIN	Actin, gamma-enteric smooth muscle OS=Bos taurus GN=ACTG2 PE=2 SV=1	2.2
ADA_BOVIN	Adenosine deaminase OS=Bos taurus GN=ADA PE=1 SV=3	2.3
SNTA1_BOVIN	Alpha-1-syntrophin OS=Bos taurus GN=SNTA1 PE=2 SV=1	5.5
AP2M1_BOVIN	AP-2 complex subunit mu OS=Bos taurus GN=AP2M1 PE=1 SV=1	3.5
CALM_BOVIN	Calmodulin OS=Bos taurus GN=CALM PE=1 SV=2	2.6
COMT_BOVIN	Catechol O-methyltransferase OS=Bos taurus GN=COMT PE=2 SV=1	3.5
CHLE_HORSE	Cholinesterase OS=Equus caballus GN=BCHE PE=1 SV=1	−6.1
CFTR_LOXAF	Cystic fibrosis transmembrane conductance regulator OS=Loxodonta africana GN=CFTR PE=3 SV=1	−2.3
DPP6_BOVIN	Dipeptidyl aminopeptidase-like protein 6 OS=Bos taurus GN=DPP6 PE=1 SV=1	3.6
RN220_BOVIN	E3 ubiquitin-protein ligase RNF220 OS=Bos taurus GN=RNF220 PE=2 SV=1	3.6
FACR2_BOVIN	Fatty acyl-CoA reductase 2 OS=Bos taurus GN=FAR2 PE=2 SV=1	6.7
GBRR2_BOVIN	Gamma-aminobutyric acid receptor subunit rho-2 OS=Bos taurus GN=GABRR2 PE=2 SV=4	5.5
IL15_BUBBU	Interleukin-15 OS=Bubalus bubalis GN=IL15 PE=2 SV=1	5.6
IL2_CEREL	Interleukin-2 OS=Cervus elaphus GN=IL2 PE=2 SV=1	5.6
IL4_BUBBU	Interleukin-4 OS=Bubalus bubalis GN=IL4 PE=2 SV=1	5.6
K1C10_BOVIN	Keratin, type I cytoskeletal 10 OS=Bos taurus GN=KRT10 PE=3 SV=1	5.6
K1C14_BOVIN	Keratin, type I cytoskeletal 14 (Fragment) OS=Bos taurus GN=KRT14 PE=2 SV=1	5.5
K1C15_SHEEP	Keratin, type I cytoskeletal 15 OS=Ovis aries GN=KRT15 PE=2 SV=1	5.6
K1C17_BOVIN	Keratin, type I cytoskeletal 17 OS=Bos taurus GN=KRT17 PE=2 SV=1	5.5
KT222_BOVIN	Keratin-like protein KRT222 OS=Bos taurus GN=KRT222 PE=2 SV=1	5.5

Gene Ther. Author manuscript; available in PMC 2016 March 01.

Accession #	Description	Fold-Change (AQP1-treated/Baseline)
KIF22_BOVIN	Kinesin-like protein KIF22 OS=Bos taurus GN=KIF22 PE=2 SV=2	3.5
PERL_BOVIN	Lactoperoxidase OS=Bos taurus GN=LPO PE=1 SV=1	3.3
TRFL_BUBBU	Lactotransferrin OS=Bubalus bubalis GN=LTF PE=1 SV=1	3.3
MAP2_BOVIN	Methionine aminopeptidase 2 OS=Bos taurus GN=METAP2 PE=2 SV=1	2.2
MYLK_SHEEP	Myosin light chain kinase, smooth muscle (Fragment) OS=Ovis aries GN=MYLK PE=2 S	2.1
PARP1_BOVIN	Poly [ADP-ribose] polymerase 1 OS=Bos taurus GN=PARP1 PE=2 SV=2	5.4
RSRC1_BOVIN	Serine/Arginine-related protein 53 OS=Bos taurus GN=RSRC1 PE=2 SV=1	2.9
NAC1_FELCA	Sodium/calcium exchanger 1 OS=Felis catus GN=SLC8A1 PE=2 SV=1	5.4
SPICE_BOVIN	Spindle and centriole-associated protein 1 OS=Bos taurus GN=SPICE1 PE=2 SV=1	5.6
SMC3_BOVIN	Structural maintenance of chromosomes protein 3 OS=Bos taurus GN=SMC3 PE=1 SV=1	5.3
STX17_BOVIN	Syntaxin-17 OS=Bos taurus GN=STX17 PE=2 SV=1	2.2
TFR1_HORSE	Transferrin receptor protein 1 OS=Equus caballus GN=TFRC PE=2 SV=1	3.6
TAGL_BOVIN	Transgelin OS=Bos taurus GN=TAGLN PE=1 SV=4	3.5
ZNHI1_BOVIN	Zinc finger HIT domain-containing protein 1 OS=Bos taurus GN=ZNHIT1 PE=2 SV=1	3.5
ZN184_BOVIN	Zinc finger protein 184 OS=Bos taurus GN=ZNF184 PE=2 SV=1	3.5